

Grassland coverage and biomass estimation based on major quadrat from UAV photogrammetry

BAO Nisha¹, LIU Shanjun¹, MAO Yachun

(1. Institute for Geo-informatics & Digital Mine Research, Northeastern University, Shenyang 110819, China; 2. Science and Technology Innovation Center of Smart Water and Resource Environment, Northeastern University, Shenyang 110819, China)

Abstract: To investigate the potential ability of unmanned aerial vehicle (UAV) in the estimation of grassland coverage and its relation to the biomass, in this study, the UAV of Phantom 3 Professional was used to acquire major quadrat with 60 m×60 m from Hulunbuir pasture land. The Wiener filtering and wavelet transformation methods were applied to de-noise UAV imagery. The imagery was further enhanced by histogram equalization. Furthermore, the excess green index and the color index were both calculated for image segmentation. The genetic algorithm based on the maximum entropy was used to estimate the grassland vegetation cover from the segmented UAV imagery. Finally, the field survey data was used to assess the accuracy of estimated vegetation coverage based on the T-test. The results showed that the maximum entropy-genetic model using excess green index from UAV imagery achieves high accuracy for grassland coverage estimation with p-value=0.8536, RMSE=6.6356. The biomass model based on variables of both height and vegetation cover performs better with accuracy of 83.41%, R² of 0.8536 and RMSE of 2.3320 g/m² hat based on a single variable of either height or vegetation. The research reveals that UAV imagery with maximum entropy-genetic model can not only provide quick, accurate, efficient ground data for vegetation monitoring, but also ground verification for vegetation estimation from remote sensing data.

Keywords: grassland coverage; biomass; UAV; major quadrat; maximum entropy; genetic algorithm

0. Introduction

The Fractional Vegetation Cover (FVC) is the percentage of the vegetation vertical projection area on the ground to the total area of the study area, which is an important parameter to show the quality of terrestrial vegetation and the growth dynamics of various plants with a certain density. Grassland biomass can be used to evaluate productivity of grassland ecosystem, grassland growth and its yield. Vegetation coverage is an important indicator to estimate biomass. Therefore, it is great significance to monitor grassland vegetation coverage and biomass which can reveal the distribution of grassland vegetation and its spatial variation law, and for provide scientific basis for grassland animal husbandry. There are meadow grassland, typical grassland, desert grassland and so on in northern China, and the grassland biomass is affected by climate, grazing, reclamation, mining and other factors. Therefore, monitoring Grassland Biomass in North China can evaluate the ability and productivity of the grassland ecosystem about obtain energy, which has scientific guiding significance for protecting grassland resources and improving grassland yield.

Owing to the diversity of spatial resolution, spectral resolution and temporal characteristics, remote sensing has become the main method to monitor regional and global vegetation coverage. However, in remote sensing estimation methods of vegetation coverage, the regression model method, classification decision tree method and artificial neural network method not only have to measure the vegetation coverage on the ground, but also require the measured data on the ground to verify the accuracy of the model further. However, vegetation index method and pixel decomposition model method only need the measured data on the ground for further verification. At present, due to the rapid development of digital photography technology, the combination of digital camera and digital image processing technology has been widely used in estimating vegetation coverage on the ground

because of its high efficiency, high speed, low price and high quality. ^[1]. UAV Remote Sensing System (UACSS) can not only make up for the inability of satellite optical remote sensing to acquire remote sensing data due to the influence of time resolution and weather, but also overcome the shortcomings of small range and time-consuming of ground remote sensing ^[2]. Compared with the previous use of optical satellite remote sensing data as data source to monitor vegetation coverage, the combination of UAV remote sensing platform and optical satellite remote sensing technology has obvious advantages ^[3]. Torres-Sanchez Studied the multi-temporal mapping of wheat field vegetation coverage based on normalized green-red difference index^[4], OVER-GREEN index, color index, vegetation index, over-green-red difference index and Woebbecke index, he tested that the estimation accuracy of the over-green index is the highest.in them.(The accuracy range is 87.73%-99% when flying at 30 m and 83.74%-87.82% when flying at 60 m). Therefore, UAV can provide large sample data for remote sensing estimation of vegetation coverage, improve the accuracy of vegetation coverage estimation model and model validation, and then estimate grassland aboveground biomass through vegetation coverage.

This study Obtain the aerial image data of the large sample by the drone, and then denoise the data of the drone by using the switch median filtering and Wiener filtering. The histogram equalization is used to perform image enhancement and other preprocess , finally use the maximum entropy method based on genetic algorithm to segment the vegetation and background in the image to estimate the vegetation coverage. Obtaining the sample around the large sample with the ground digital camera to verify the result. And analyzing the correlation between vegetation coverage and biomass estimated by digital camera. Established a foundation for the application of UAV remote sensing platform and optical satellite to estimate the vegetation coverage of Hulunbuir grassland, and provided a scientific basis for large-area ground data and remote sensing technology to monitor grassland biomass and growth.

1.Study area and dataset

1.1 Study area

The study area is located in the middle of the Hulun Buir grassland in Inner Mongolia (Figure 1). The climate type is arid and semi-arid, and the precipitation is mainly concentrated in July and August. The grassland-using type is meadow grassland, and the grassland utilization methods mainly include fenced grassland, grazing grassland, and degraded grassland. The grassland plant community consists mainly of *Potentilla acaulis* L., *Artemisia gmelinii*, *Artemisia annua* Linn., *Brassica juncea*(L.)Czern. et Coss., *Leymus chinensis*, *Stipa capillata* Linn and so on always have high vegetation coverage. Due to human activities such as reclamation, grazing and mining, some grassland degradation and desertification have occurred in the study area.

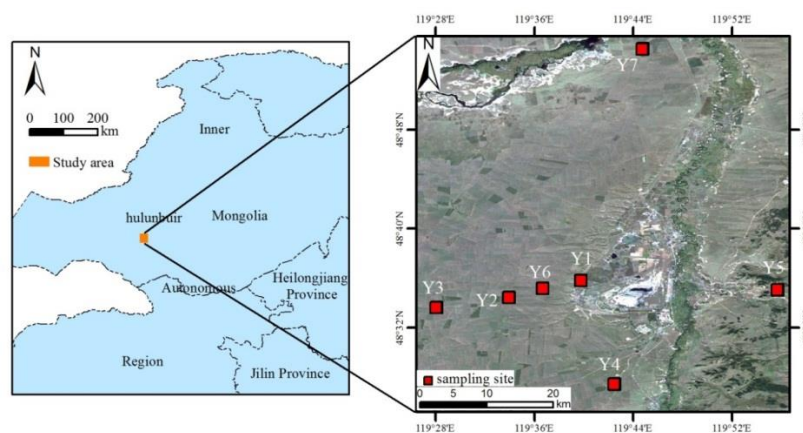


Fig.1 Location of the research area and sampling

1.2 Sampling method and data

Ground sampling and observation experiments were carried out on the study area from July 12 to 14, 2016. The sample was selected according to the composition of the grassland plant community, grazing, degradation and topographic conditions. The terrain condition is based on the partition random sampling method. The position of the sample is selected to be uniform in the grassland in a certain area around it, and the vegetation landscape is consistent. The location of the sampling points is shown in Figure 1. The schematic diagram of the layout of the plot is shown in Figure 2. The size of the unmanned aerial vehicle is set to 60 m × 60 m. The Dhan Phantom 3 Profession UAV (parameters shown in Table 1) flies about 100 m above the sample side to obtain the remote sensing data of the drone aerial photography. At the same time, nine 1 m × 1 m sample squares were placed around the large sample of the drone, and the data was taken vertically by 1 m above the Sony SELP 1650 digital camera. Using GPS to record the geographic coordinates of each sample, and the plant community type and geomorphological environment within the sample (Table 2), and harvest all the vegetation within the 1 m × 1 m sample to remove the debris and other impurities. The object is loaded into the bag and marked. Finally, a total of 7 large sample squares and 63 small sample squares are obtained. The bags filled with vegetation were taken back to the laboratory, dried at 80 ° C to constant weight, and then weighed with an electronic balance with an accuracy of 0.01 to obtain the total amount of organic matter per unit area, which is biomass.



Fig.2 Sketch map of sample plot

Tab.1 Parameters of DJ Phantom 3 Profession

Parameter	Value
Model type	Four-rotor aircraft
Battery Type	LiPo4S
weight	1280g
Diagonal distance (including OARS)	590mm
flight height	500m
Working Environment Temperature	0°C-40°C
Support memory card type	Micro-SD card
Photo maximum resolution	4000x3000
Electronic shutter speed	8 seconds - 1/8000 seconds
Bands	Red Band、Green Band、Blue Band

Tab.2 Landscapes and vegetation types in the sample plot

Sample area	Landform type and land use	Vegetation types
Y1	Low-lying land: it is distributed in low-lying river valley terraces, with salinization and low, grass cover and yield	<i>Iris ensata</i> Thunb. <i>Carex duriuscula</i> C.A.Mey. <i>Hordeumbogdanii</i> Wilensky- <i>Cleistogenes squarrosa</i> (Trin.) Keng
Y2	Hilly plain: it is distributed in a flat land with an elevation of about 700m, with high quality grazing land with a few types of vegetation	<i>Stipa baicalensis</i> - <i>Leymus chinensis</i> .
Y3	Wavy plain: which distributed in the inter-hill flat, is a high quality grazing and mowing grassland	<i>Leymus chinensis</i> - <i>Achnatherum sibiricum</i>
Y4	Wavy plain: the terrain is a wavy plain, not very flat, and small relief, high grassland coverage	<i>Leymus chinensis</i> - <i>Stipa baicalensis</i>
Y5	Low hills: large terrain relief, meadow grassland, easy to desert	<i>Stipa baicalensis</i> - <i>Carex tristachya</i>

Y6	Low ground: sandy bare land	<i>Leymus chinensis</i> - <i>Agropyron cristatum</i> (Linn.) <i>Gaertn.-Artemisia desertorum</i> Spreng. Syst. Veg.- bunch grass
Y7	Valley depression: saline soil	<i>Leymus chinensis</i> - <i>Stipa capillata</i> Linn.

2 Methods

2.1 UAV data preprocessing

2.1.1 UAV image denoising

Due to the influence of the sample environment and the UAV's own communication, the UAV will be interfered by impulse noise and Gaussian noise during the aerial photography and image transmission. There are spikes in the histogram and the gray value. The position of 0 and 255 has noise effects, which will affect the accuracy of vegetation coverage extraction. Therefore, the image needs to be denoised before the vegetation coverage is extracted. If a denoising method is adopted, the effect of noise cannot be completely eliminated. This paper uses switch median filtering to eliminate impulse noise, and uses Wiener filtering based wavelet transform to eliminate the remaining Gaussian noise basing on this situation.

The Wiener filtering based wavelet transform denoising step (Figure 3) is as follows:

- (1) Using the first-order wavelet decomposition on the image of the drone that removes the impulse noise, respectively obtaining LL, LH, HL, HH;
- (2) Since most of the original information is retained in the LL, the denoising process is not performed, and the LH, HL, and HH are denoised by the Wiener filter;
- (3) Performing wavelet reconstruction on LL, LH, HL, and HH to obtain a denoised image

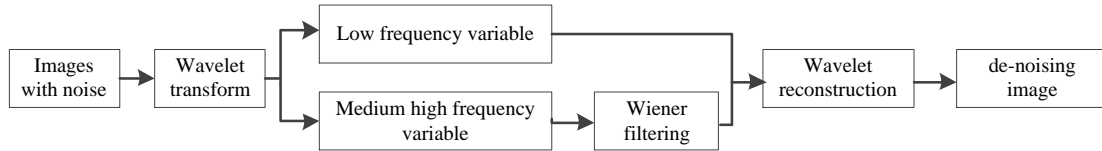


Fig.3 Flow chart of wavelet transform based on wiener filtering

2.1.2 UAV image enhancement

In this paper, the histogram equalization is used to enhance the image of the drone, highlight the grassland vegetation information and suppress the soil background information. Histogram equalization is a function of the cumulative distribution function of each gray level probability of the image as a transform function. Obtaining an image with uniform distribution of gray probability density after transformation to enhance the contrast of the image, the cumulative distribution function can be expressed as:

$$s_k = T(r_k) = \sum_{j=0}^k \frac{n_j}{n} = \sum_{j=0}^k p_r(r_j), \quad 0 \leq r_j \leq 1, \quad k = 0, 1, \dots, L-1$$

2.2 Extracting Vegetation Coverage Based on Maximum Entropy-Genetic Algorithm

The maximum entropy method transforms the image segmentation into mathematical optimization by establishing the objective function of vegetation and background, and then uses the genetic algorithm to find the optimal segmentation threshold. The process of extracting vegetation coverage by the maximum entropy method based on genetic algorithm is shown in Fig. 4.

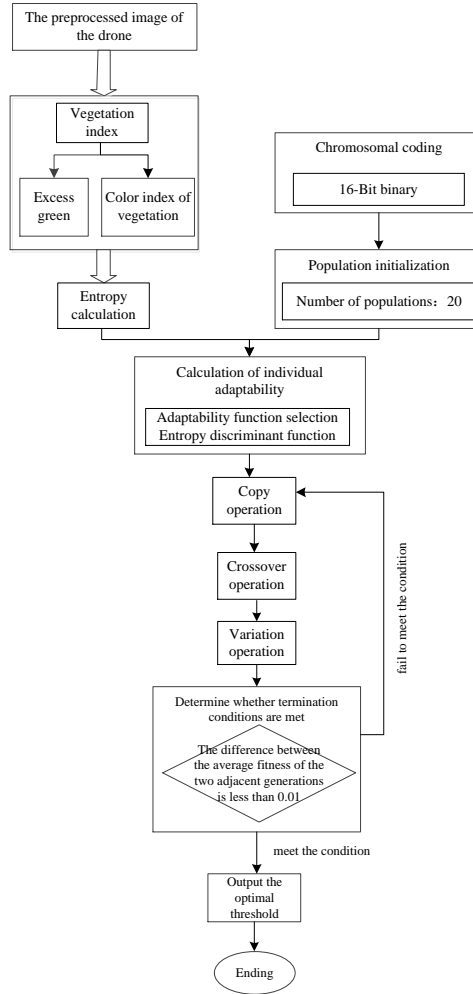


Fig.4 Flow chart of estimating vegetation coverage based on maximum entropy and genetic algorithm

The main steps are as follows:

(1) Calculating the vegetation index: Since the data obtained by the drone is only three bands of red, green and blue, the calculation of the color difference between the vegetation and the background (bare soil, shadow, sandstone, etc.) selects the commonly used green index and color index. And make corrections.

Over-green vegetation index [5] (Excess green,) calculation formula:

$$\text{When } g > r \text{ and } g > b: \text{Exg} = 2 \times g - r - b \quad (2)$$

Otherwise $\text{Exg} = 0$.

Color index of vegetation, CIVE calculation formula:

When $g > r$ and $g > b$:

$$\text{CIVE} = 0.441 \times r - 0.881 \times g + 0.385 \times b + 18.78745 \quad (3)$$

Otherwise $\text{CIVE} = 0$.

The r , g , b are the red band, green band and blue band in the aerial image of the drone.

(2) Calculation of entropy: According to the principle of maximum entropy algorithm, the discriminant function of entropy is calculated as follows: The set of gray values in the vegetation index image is $\{0, 1, 2, \dots, 255\}$, which has N pixels. The number of pixels with gray value i is represented by $\varphi(i)$, and the probability is represented by $p(i)$, which is:

$$p(i) = \frac{\varphi(i)}{N}, \quad i = 1, 2, \dots, 255 \quad (4)$$

When image segmentation of vegetation index constructed by UAV images is carried out, the red and blue bands are larger than the green band due to the influence of humidity. Therefore, the image segmentation categories are divided into vegetation, background, and affected by bare soil. The three types of vegetation are $\{C_1, C_2, C_3\}$, $\{0, 1, \dots, G_1\}$, and the gray values corresponding to each category are $\{G_1 + 1, G_1 + 2, \dots, G_2\}, \dots, \{G_2 + 1, G_2 + 2, \dots, 255\}$, then there are 2 thresholds, which are $\{T_1, T_2\}$

The probability of the gray value corresponding to each category is:

$$C_1: \frac{p_0}{P_1}, \frac{p_1}{P_1}, \dots, \frac{p_{G_1}}{P_1}, \quad C_2: \frac{p_{G_1+1}}{P_2}, \frac{p_{G_1+2}}{P_2}, \dots, \frac{p_{G_2}}{P_2}, \quad C_3: \frac{p_{G_2+1}}{P_3}, \frac{p_{G_2+2}}{P_3}, \dots, \frac{p_{255}}{P_3} \quad (5)$$

Which $P_k = \sum_{i \in C_k} p_i, k = 1, 2, \dots, 3$.

Thus, the entropy of each category is:

$$E_k = - \sum_{i \in C_k} \frac{p_i}{P_k} \log \frac{p_i}{P_k} = \log P_k - \sum_{i \in C_k} p_i \log p_i \quad (6)$$

The discriminant function that defines entropy is:

$$Entory(T_1, T_2,) = \sum_{k=1}^3 E_k \quad (7)$$

When the amount of information of the target and the background is the largest, the segmentation threshold when the discriminant function of the entropy is the largest is obtained, namely:

$$(T_1^*, T_2^*) = \arg \max \sum_{k=1}^3 E_k \quad (8)$$

(3) Coding: The vegetation index calculated by the UAV image has a gray value between 0 and 255. At the same time, the image is segmented using two thresholds, so the encoding is performed with 16-bit binary.

(4) Set the initial population: the number of populations is set to 20 and the breeding algebra is 100.

(5) Design fitness function: The fitness function selects the discriminant function of entropy. By generating the random number as the initial segmentation threshold, the fitness of each individual is calculated.

(6) Copy: The copying operation uses the roulette method to inherit the chromosomes of the individuals of the previous generation with high fitness to the next generation through the copying operation.

(7) Intersection: The crossover probability is set to 0.6, and the crossover operation uses a two-point crossover. Cross-operation will result in a more adaptable individual, which can speed up the overall optimization.

(8) Variation: The probability of variation is 0.03, preventing the population from stopping the evolution by obtaining the optimal segmentation threshold at the beginning.

(9) Termination conditions: When the difference between the average fitness of two adjacent generations is less than 0.01, the evolution tends to be stable, or the evolution is completed when the maximum number of iterations is reached.

3 Results and analysis

3.1 UAV data preprocessing results

Taking Y5 as an example, the image of the drone image is denoised by the switch median filtering and the wavelet transform based on Wiener filtering. The image histogram after denoising is shown in Fig. 5. The results show that after the image of the drone is denoised, the histogram is smoother and there is no value at the gray value of 0 and 255, which eliminates the influence of noise on the image. The histogram equalization is used to enhance the image of the denoised drone image, and the histogram before and after the enhancement (Fig. 5) and the image before and after the enhancement (Fig. 6) are displayed. After the image of the drone is equalized, each gray scale is obtained. The grade distribution is relatively uniform, and the difference between vegetation and soil background is obvious.

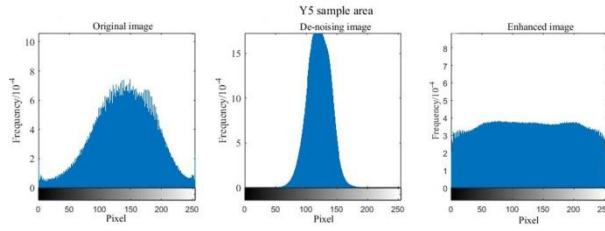


Fig.5 Histogram of preprocessed UAV image

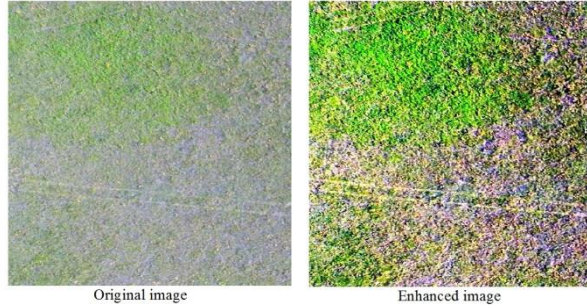


Fig.6 UAV image enhancement

3.2 UAV vegetation coverage extraction results and verification

The pre-processing of the UAV sample data and the calculation of the vegetation index were carried out. The maximum entropy method based on genetic algorithm was used to extract the vegetation coverage. The results are shown in Table 3. The results show that the vegetation coverage results, threshold value 1, and threshold 2 estimated by the two vegetation indices are different, and the maximum entropy difference is not large.

Tab.3 The result of estimating vegetation coverage

Sample plot	Vegetation index	FVC(%)	Threshold 1	Threshold 2	Maximum entropy
Y1	Excess green	16.03	2	159	8.97
	Color index	14.27	9	153	9.03
Y2	Excess green	32.16	20	103	9.46
	Color index	25.06	11	131	9.37
Y3	Excess green	28.19	5	148	9.49
	Color index	24.27	3	135	9.34
Y4	Excess green	32.31	19	123	9.62
	Color index	28.49	7	125	9.41
Y5	Excess green	30.52	4	134	9.61
	Color index	34.28	9	133	9.48
Y6	Excess green	26.89	2	193	9.09
	Color index	21.99	6	115	9.19
Y7	Excess green	31.25	1	119	9.44
	Color index	30.18	6	147	9.29

In order to quantitatively analyze the accuracy of grassland vegetation coverage, the control points of hand-held GPS are used to geometrically correct the image of the drone, and the position of the control point is obtained by the field photography method. Vegetation coverage (Fig. 7), According to the T-test method, the vegetation coverage of the 1 m×1 m sample was estimated by the photographic method to verify the UAV image estimation results, and the root mean square error was calculated. Based on the estimation of vegetation coverage by drones and the estimation of vegetation coverage by the photographic method, the T test results are shown in Table 4. There is no significant difference between the estimation results of the two vegetation indices of the UAV

image and the photographic estimation results ($P < 0.05$). Among them, the accuracy of the over-green index is higher. The T-test P value is 0.272 and the root-square root error is 6.6356. This method can be used to estimate the vegetation coverage of the drone.

Among the seven plots, the precision of Y6 sample plot is the highest and that of Y2 sample plot is the lowest. Then, the Y6 plot is low-lying land of hilly land and sandy bare soil. The vegetation type is small and the coverage is low, while Y2 is a hilly flat land with many vegetation types, high coverage and strong spatial heterogeneity, which leads to Y2 plot. The estimation accuracy is lower than other plots (Table 5).

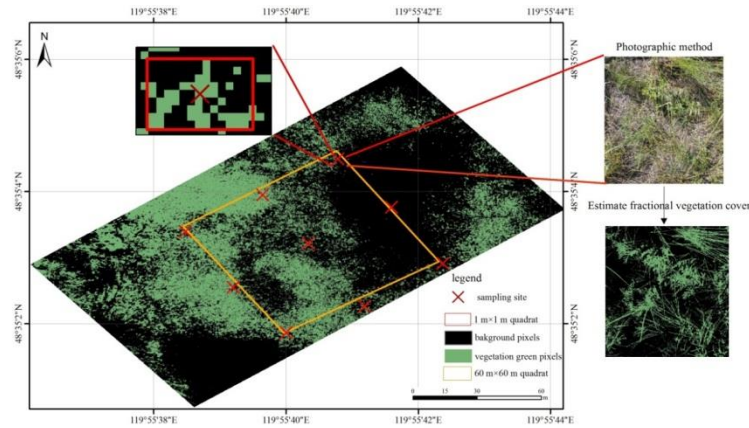


Fig.7 Verification sketch map of large quadrat

Tab.4 Precision of estimating vegetation coverage by UAV image

Vegetation Index	p-value	RMSE
Excess green	0.272	6.6356
Color index	0.068	6.8887

Tab.5 RMSE of estimating vegetation coverage by UAV imagery form various sampling plot

Sample area	Excess green	Color index of vegetation
Y1	2.1218	2.4721
Y2	11.8169	12.3277
Y3	8.6951	2.8827
Y4	3.9878	5.1246
Y5	2.9042	2.3931
Y6	1.9217	2.0563
Y7	2.3605	2.4215

3.3 Correlation analysis between vegetation coverage and biomass

Due to biomass is closely related to vegetation coverage (P), vegetation height (h), and product of vegetation coverage and plant height (Ph) [7], this paper deals with grassland biomass and three variables. The correlation between the two was analyzed. The results are shown in Table 6. There is a significant correlation between biomass and three variables, and the correlation coefficient is above 0.8. The correlation between biomass and vegetation coverage and plant height is shown and the highest is 0.9134.

Tab.6 correlation coefficient of grassland biomass with each variable

Type	P	h	$P \times h$
Grassland biomass	0.9075	0.8016	0.9134

In this paper, the regression equations such as $y = a + bx$, $y = ax^b$, $y = ax^2 + bx + c$, $y = ax^3 + bx^2 + cx + d$, $y = a + blgx$ were modeled by the biomass and single variables P , h , the cross-variable Ph product and

the joint variables P and h. The root mean square error and estimation accuracy were calculated to analyze the accuracy of each model.

$$RMSE = \sqrt{\frac{\sum_{i=1}^n (AGR_i - AGR'_i)^2}{N}} \quad (9)$$

$$Ac = \left(1 - \frac{RMSE}{\overline{AGR}}\right) \times 100\% \quad (10)$$

Where RMSE is the root mean square error, AGR_i is the measured grassland biomass, AGR'_i is the estimation of grassland biomass, N is the number of samples, Ac represents the estimation accuracy, and \overline{AGR} represents the average of the measured grassland biomass value.

The fitting results and precision are shown in Table 7. As shown in Figure 8, in the single variable, the best fit between biomass and variable P and biomass and variable h is the cubic regression model, where the combined effect of the variable P is three times. (R2 is 0.8244, RMSE is 3.5008 g/m2, and the estimation accuracy is 78.80%), which is better than the variable h three-time fitting (R2 is 0.7460, RMSE is 3.6213 g/m2, and the estimation accuracy is 76.42%). The cross-variable Ph and the joint variables P and h are better than the single-variable modeling accuracy. For the joint variables P and h, the fitting effect is once (R2 is 0.8326, RMSE is 2.6119 g/m2, and the estimation accuracy is 82.26%). Compared with the best fit of a single variable, the cross-variable Ph three-regression modeling has the highest accuracy (R2 is 0.8536, RMSE is 2.4420 g/m2, and the estimation accuracy is 83.41%).

Tab.7 The model and precision of grassland biomass and every variable

Variable	Equation	R ²	RMSE(g/m ²)	Estimation accuracy
Vegetation coverage (P)	$y=40.2945 \times P+5.5763$	0.8204	3.5398	78.57
	$y=42.9199 \times P^{0.7059}$	0.8011	3.7470	77.07
	$y=4.9560 \times P^2+36.0517 \times P+6.1845$	0.8215	3.5291	78.63
	$y=42.6549 \times P^3-51.4058 \times P^2+54.6344 \times P+4.7378$	0.8244	3.5008	78.80
	$y=31.3091+22.2031 \times \lg P$	0.6446	4.9800	69.85
Height of plant (h)	$y=0.9347 \times h-1.4956$	0.6355	4.3379	71.75
	$y=0.4529 \times h^{1.2091}$	0.6547	4.2500	71.98
	$y=0.0389 \times h^2-0.6454 \times h+12.8372$	0.7208	3.7965	75.28
	$y=0.0029 \times h^3-0.1415 \times h^2+2.8060 \times h-7.0028$	0.7460	3.6213	76.42
	$y=-27.2861+34.6656 \times \lg h$	0.5184	4.9862	67.53
Product of Vegetation coverage and Height of plant (Ph)	$y=1.0919 \times Ph+9.3038$	0.8308	2.6257	82.16
	$y=7.6991 \times Ph^{0.4594}$	0.8177	2.7491	81.14
	$y=-0.0156 \times Ph^2+1.5226 \times Ph+8.0081$	0.8462	2.5029	83.00
	$y=0.003 \times Ph^3-0.1251 \times Ph^2+2.2776 \times Ph+6.9837$	0.8536	2.4420	83.41
	$y=7.8212+13.19 \times \lg Ph$	0.6471	3.7922	74.24
Vegetation coverage (P) Height of plant (h)	$y=26.959 \times P+0.3403 \times h+2.1430$	0.8326	2.6119	82.26

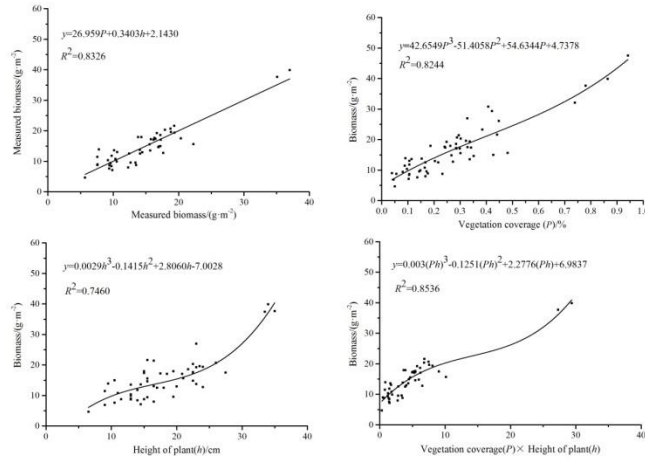


Fig.8 Fitting result of grassland biomass and each variable

4. Conclusion

In this paper, UAV is used to obtain 60 m×60 m large sample data of Hulunbuir meadow grassland to process, analyze and verify the UAV images and estimate the vegetation coverage and grassland biomass in the sample. The following conclusions are as follows:

(1) Using genetic algorithm to optimize the vegetation and background maximum entropy objective function, and obtain the dynamic segmentation threshold of vegetation and background in each plot image to get the vegetation coverage, combining with field synchronization field data, according to the T test to verify the accuracy of the root mean square error. The results show that the proposed method has higher estimation accuracy (T test P value is 0.272, root mean square error is 6.6356).

(2) The correlations among the grassland biomass and vegetation coverage, vegetation plant height and grassland vegetation coverage and plant height were high, and the correlation between biomass and vegetation coverage was the highest, which is 0.9134. The constructed cross-variable Ph three-regression method is higher than the single variable. (R2 is 0.8536, RMSE is 2.4420, and the estimation accuracy is 83.41%).

Reference

- [1] ZHANG Dongdong, MANSARAY Lamin R., JIN Hongwei, et al. 2018. A universal estimation model of fractional vegetation cover for different crops based on time series digital photographs[J]. Computers and Electronics in Agriculture, 151: 93-103.
- [2] ANGUIANO-MORALES Marcelino, CORRAL-MARTÍNEZ L. F., TRUJILLO-SCHIAFFINO Gerardo, et al. 2018. Topographic investigation from a low altitude unmanned aerial vehicle[J]. Optics and Lasers in Engineering, 110: 63-71.
- [3] SENTHINATH J, KANDUKURI Manasa, DOKANIA Akanksha, et al. 2017. Application of UAV imaging platform for vegetation analysis based on spectral-spatial methods[J]. Computers and Electronics in Agriculture, 140: 8-24.
- [4] TORRES-Sánchez J, Peña J M, DE CASTRO A I, et al. 2014. Multi-temporal mapping of the vegetation fraction in early-season wheat fields using images from UAV[J]. Computers & Electronics in Agriculture, 103(2):104-113.
- [5] WOEBBECKE D M, MEYER George E, BARGEN K Von, et al. 1995. Color Indices for Weed Identification Under Various Soil, Residue, and Lighting Conditions[J]. Transactions of the Asae, 38(1): 259-269.
- [6] NAHVAR JoseH, NAHJERA Juan, JURADO Enrique. 2002. Biomass estimation equations in the Tamaulipan thornscrub of north-eastern Mexico[J]. Journal of Arid Environments, 52(2):167-179.
- [7] WEN Zhaofei, MA Maohua, ZHANG Ce, et al. 2017. Estimating seasonal aboveground biomass of a riparian pioneer plant community: An exploratory analysis by canopy structural data[J]. Ecological Indicators, 83: 441-450.